Egypt. J. Chem. **Vol. 60**, No. 4, pp. 697 - 710 (2017)

Synthesis, Characterization and Performance Evaluation of Lithium Manganese Oxide Spinels for Lithium Adsorption

M. H. Sorour[1], Heba A. Hani[1,*], Mayyada M.H. El-Sayed[1,2] , Amany A. Mostafa[3] and Hayam F. Shaalan[1]

[1]Chemical Engineering and Pilot Plant Department, National Research Centre, [2]Chemistry Department, American University in Cairo, AUC Avenue, New Cairo 11835 and [3]Department of Ceramics, National Research Centre, EL Bohouth st., 12622 Dokki, Cairo, Egypt.

The recovery of lithium from seawater via adsorption is a promising separation technique that could be incorporated within integrated salt recovery schemes. In this work, spinel-type manganese oxide adsorbents were prepared and utilized for selective lithium adsorption from synthetic solutions. The semi-dry solid-state method was adopted to prepare spinel-type ion sieves using different manganese and lithium sources; manganese carbonate, manganese oxide, lithium carbonate and lithium hydroxide. Synthesis was conducted at different Li/Mn starting molar ratios, firing temperatures and firing durations. The prepared spinels were characterized by X-ray diffraction (XRD) and scanning electron microscopy (SEM). Moreover, average particle size and zeta potential were measured for selected spinel adsorbents. In addition, their sorption capacities and lithium removal efficiencies from synthetic solutions were evaluated. Lithium uptake results suggested that the spinels ($H_{1.1}Li_{0.08}Mn_{1.73}O_{4.05}$) prepared from manganese carbonate and lithium hydroxide at Li/Mn ratio of 0.75 exhibited at pH 12 the highest lithium sorption capacity among other prepared spinels. The equilibrium of lithium sorption onto this adsorbent was best described by Langmuir isotherm model and the maximum equilibrium sorption capacity was found to be 50 mg/g. This capacity was obtained using 0.25 g/L of the adsorbent at pH 12 and its value is higher than previously reported values. Thus, the prepared spinel shows promising features that favor its utilization for lithium removal from wastewater and concentrated brines.

Keywords: A. synthesis, D. manganese oxide spinels, E. lithium selective adsorbents, E. equilibrium adsorption.

Introduction

The distinguished properties of lithium have deemed it attractive for various applications such as lithium ion batteries, nuclear fusion fuels, light weight aircraft alloys and manufacture of ceramics, glass, and lubricants, in addition to pharmaceutical compounds necessary for drug delivery [1, 2]. Terrestrial and marine sources of lithium are not abundant. Lithium ion reserves in seawater amount to approximately 2.5×10^{14} Kg, and its concentration ranges between 0.1-0.2 ppm [3-5].

Various technologies have been adopted for lithium recovery from seawater and desalination brines and these include, but are not limited to, membrane processes using nanofiltration (NF) and reverse osmosis (RO) [2, 6-8], precipitation [9], adsorption [10, 11] or a combination thereof [12]. Adsorption proved to be a promising method for lithium recovery due to its high efficiency, selectivity, reproducibility and operability for scale-up. The majority of the reported adsorption studies utilized inorganic adsorbents based on manganese oxide in the form of nanocrystal ion sieves [13], nanorods [14], and spinels [15, 16] . Hydrous manganese oxide spinels were also blended with polymers such as polyacrylonitrile (PAN) and polyvinyl chloride (PVC) to obtain PAN-$H_{1.6}Mn_{1.6}O_4$ and PVC-$H_{1.6}Mn_{1.6}O_4$ Li ion sieve membranes, respectively. At equilibrium, the former removed 10.7 mg/g of lithium from simulated seawater desalination retentate at pH 11 [17] , while the latter sorbed 36.77 mg/g from

*Corresponding author e-mail: hi_heba2@yahoo.com, Tel: +201005276183
DOI : 10.21608/ejchem.2017.4170

an aqueous synthetic lithium chloride solution at pH 12 [18]. In addition Few studies used other inorganic and polymeric adsorbents. Titania ion sieves were employed and sorption capacities up to 25 mg/g were obtained at pH 9 [19]. Maximum sorption capacities obtained by commercial adsorbents of Amberlite IR 120 Na, Amberlite IR 120 H and Molecular Sieve 13X were 22, 20 and 25 mg/g, respectively at pH 7 [20]. MnO_2 nanorods and nanocrystals exhibited lithium sorption capacities ranging from 17.8 to 45 mg/g [13, 14, 21].

Amongst all the investigated lithium adsorbents, manganese oxide based adsorbents are considered the most promising lithium adsorbent materials [11, 22-24] . Maximum reported lithium sorption capacities from synthetic or saline solutions for the different types of manganese oxide spinel types ranged from 12 mg/g to 45 mg/g, depending on the spinel structure, preparation method and employed sorption conditions [3, 11, 15, 16, 23, 25-27]. Spinels are generally prepared via hydrothermal, emulsion or solid state reaction techniques, in addition to other methods such as electrospinning [28-30]. It was concluded from reported literature that Li/Mn mole ratio as well as heating/firing temperatures have major impact on lithium uptake [23].

This work aims at synthesizing a novel high lithium uptake capacity adsorbent to be used for Li recovery from seawater. This is achieved through investigating the effect of different spinel synthesis conditions on lithium sorption capacity in order to obtain a selective adsorbent with high performance efficiency. In this regard, the semi-dry solid-state method was adopted for the preparation of spinel Li-Mn oxides using various manganese and lithium sources, at different Li/Mn starting molar ratios, firing temperatures and durations. Morphology, structure, zeta potential, particle size and performance of the prepared adsorbents were also evaluated. The adsorbent with the best performance was selected for further isotherm investigations for the determination of the maximum adsorption capacity.

Materials and Methods

Materials

Materials used in this study were lithium hydroxide ($LiOH.H_2O$), lithium carbonate (Li_2CO_3), lithium chloride (LiCl), manganese oxide (MnO_2) from (Loba Chemie, India), manganese carbonate ($MnCO_3$) (Fluka, Germany), sodium hydroxide, sodium chloride and hydrochloric acid (33%) (Fluka and Sigma Aldrich).

Methods

Synthesis of lithium manganese oxide spinels

Lithium manganese oxide spinels were prepared via a semi-dry solid-state reaction between a manganese source precursor of either MnO_2or $MnCO_3$ together with a lithium source precursor of either $LiOH{\cdot}H_2O$ or Li_2CO_3. The powdered manganese and lithium precursors were mixed at different Li/Mn molar ratios (0.75-1.5) and were ground for 15 min. The prepared spinels were divided into two groups according to the starting lithium molar ratios (group I) and to the effect of the use of the different starting precursors (group II).

Two firing regimes were adopted as presented in Fig. 1. In the first regime (firing regime "a"), the mixture was heated at 425^{o}C for 5 hr in an electric oven (LabTech) at a heating rate of 4^{o}C/min. It was then cooled for 1.5 hr at room temperature, mixed and ground again for 15 min. However, in the second firing regime (firing regime "b"), a portion of the previous mixture obtained from regime "a" was sintered at 500^{o}C for 5 hr with the same heating rate of 4^{o}C/min. Then it was slowly cooled at a rate of (1^{o}C/min) for up to 12 h. Before using the produced spinels for lithium sorption, each spinel powder was acid washed by soaking overnight in (0.5-1 M) hydrochloric acid (HCl) solution 2-3 times. Acid washing step was performed to allow for the ion-exchange between Li^+ ions in the adsorbent and H^+ ions in HCl solution in order to produce H-Mn oxide spinels with ion-exchangeable protons [26]. The volume of HCl solution was adjusted such that the molar ratio of H^+ in the solution to Li^+ in the adsorbent was more than 40 as reported in previous work [3] .

The obtained powder was then filtered using 1-micron millipore filter, washed twice with deionized water, then dried at 110^{o}C for 2hr and finally left to cool down to room temperature. The flowchart in Fig. 1 illustrates the steps pertaining to each of the two firing regimes "a" and "b". The different employed precursor combinations and synthesis conditions for the prepared spinels are compiled in Table 1. Group (I) includes the adsorbents prepared under different Li/Mn molar ratios (0.75-1.5) using the same precursors of

$LiOH.H_2O$ and MnO_2. Group (I) adsorbents are 1a, 2a, 3a, 1b, 2b and 3b, where "a" and "b" refer to the two employed firing regimes. Group (II), on the other hand, includes the adsorbents prepared using different combinations of manganese and lithium precursors at Li/Mn molar ratio of 0.75 and it is divided into two subgroups IIA and IIB. Subgroup IIA encompasses the adsorbents prepared using $LiOH.H_2O$ as the lithium-based precursor, whereas subgroup IIB encompasses those prepared using Li_2CO_3.

Characterization of the prepared adsorbents

The crystalline structures of the precursors, synthesized ion sieves and delithiated spinels were determined by X-ray phase analysis using Bruker D8 Advance with secondary monochromatic beam Cu Kα radiation at 40 Kv and 40 mA diffractometer. Morphology of the prepared adsorbents was characterized by scanning electron microscopy (SEM, Quanta FEG250) equipped with EDS, using an accelerating voltage of 15-30 kV, magnification up to 400,000 and resolution for W 3.5 nm. Average particle size and zeta-potential of the synthesized ion sieves were measured using a zeta-sizer nano series instrument (Malvern Instrument, UK) with a nano-zeta sizer of 532 nm laser wavelength.

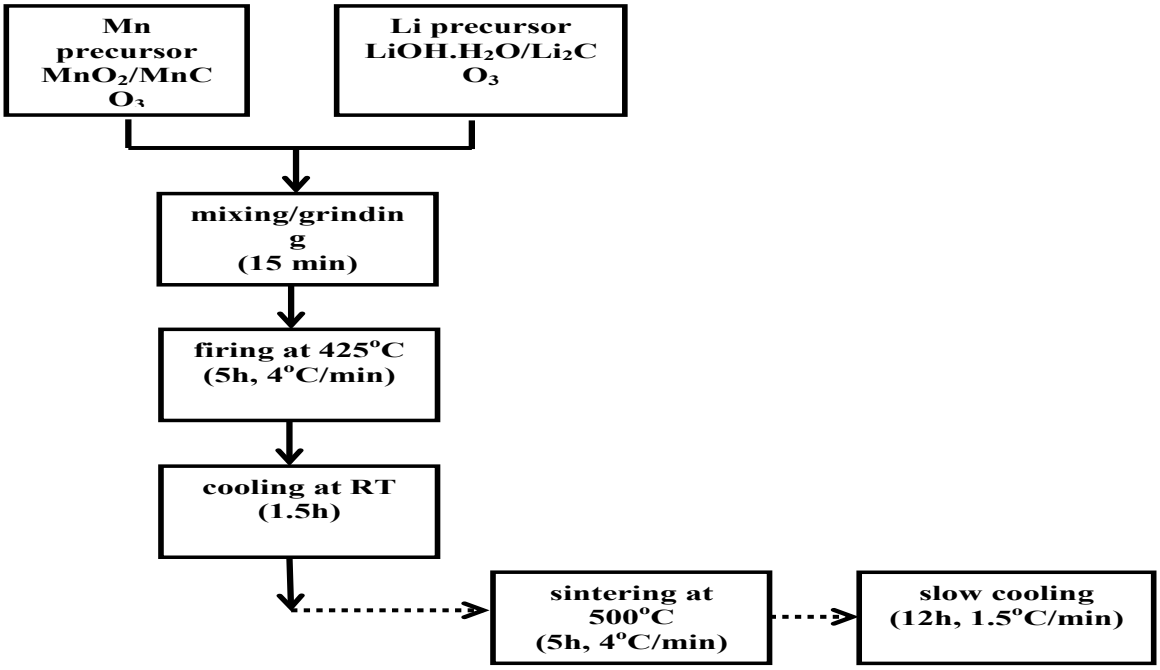

Fig. 1. Flowchart showing the steps of each of the firing regimes "a" and "b". Solid and dashed lines belong to regimes "a" and "b", respectively.

TABLE 1. Precursor combinations and synthesis conditions for the prepared lithium-manganese oxide spinel adsorbents.

Group	Adsorbent code	Li/Mn	Precursors	
I	1a, 1b	0.75	$LiOH.H_2O$	MnO_2
	2a, 2b	1.00		
	3a, 3b	1.50		
IIA	4a, 4b	0.75	$LiOH.H_2O$	MnO_2
	5a, 5b			$MnCO_3$
IIB	6a, 6b	0.75	Li_2CO_3	MnO_2
	7a, 7b			$MnCO_3$

* a: Firing regime "a": Samples fired at 425°C, 5hr.

** b: Firing regime "b": Samples fired at 425°C, 5hr followed by 500°C, 5 hr.

Performance evaluation and equilibrium studies

Batch contacting experiments were conducted in 250-500 ml flasks by adding a certain amount of each of the prepared adsorbents to a specific volume of lithium chloride synthetic solution of initial concentration 45 mg/l at a dose of 1 g/L. The pH of the mixture was adjusted to either pH 8 or 12 by using a mixed buffer solution (0.1 M) of sodium chloride and sodium hydroxide in the ratio of 2:1 by volume. Afterwards, the mixture was shaken overnight at 150 rpm and room temperature in a shaking water bath (Julabo, SW-20C). It was then filtered using 1-micron millipore filter (Whatman filter paper 42) and the supernatant was collected to be further analyzed using an atomic absorption flame spectrophotometer (AAS) type (GBC Avanta). The sorption capacity (q) was calculated by mass balance using the following equation [30].

$$q = \frac{C_o - C_e}{m} \times V \qquad (1)$$

where q is the amount of Li ions sorbed in (mg/g adsorbent), C_o and C_e are the initial and equilibrium ion concentrations (mg/L), respectively; V is the volume of saline solution used in litre (L) and m is the weight of dry adsorbent (g).

The dose effect of the spinel that possessed the highest Li sorption capacity among the other prepared ones was studied varying from 0.25-1 g/L at under the same investigated adsorption conditions.

Based on the findings of the previous sections, equilibrium isotherm experiments were performed on the selected spinel adsorbent. The adsorbent was added to each of a series of flasks containing synthetic lithium chloride solution at the selected optimum dose and pH, different initial concentrations (5-51 mg/L). All experiments were carried out in duplicates and the mean values are presented. Experimental data was fitted to Langmuir and Freundlich isotherm models. Langmuir sorption isotherm assumes monolayer surface coverage on a structurally homogeneous adsorbent having energetically identical sorption sites. The linear form of Langmuir isotherm is given by:

$$\frac{C_e}{q_e} = \frac{1}{b q_m} + \frac{C_e}{q_m} \qquad (2)$$

where C_e is the equilibrium aqueous metal ion concentration (mg/L), q_e is the amount of metal ions adsorbed per gram of adsorbent at equilibrium (mg/g), q_m and b are the Langmuir constants related to the maximum sorption (saturated monolayer) capacity and the free energy of sorption, respectively. The values of q_m (mg/g) and b (L/g) can respectively be determined from the slope and intercept of the linear plot [32-34].

Freundlich isotherm describes multilayer sorption on heterogeneous surfaces. The logarithmic form of the equation can be expressed as

$$\log(q_e) = \log(K_F) + \frac{1}{n}\log(C_e) \qquad (3)$$

where K_F is a rough indicator of the sorption capacity ((mg/g)/(L/mg)^n) and 1/n indicates sorption intensity. The magnitude of the exponent 1/n gives an indication of the favorability of sorption [32, 33, 35].

Results and Discussion

Characterization of the prepared spinels

Spinels' structure: XRD analysis

The structure of the acid washed spinels was analyzed by XRD. Figure 2 shows the XRD patterns of Group I adsorbents prepared using $LiOH.H_2O$ and MnO_2 with different Li/Mn molar ratios of 0.75, 1 and 1.5. Adsorbents prepared via firing regime "a" are (1a), (2a) and (3a) while those prepared via firing regime "b" are (1b), (2b) and (3b), respectively. The figure shows that the cubic face-centered spinel $H_{1.1}Li_{0.08}Mn_{1.73}O_{4.05}$ (as identified by XRD card no. 51-1584) was formed in all Group I adsorbents fired via both firing regimes except sample (3a) which was prepared at high Li/Mn ratio (1.5) and was fired at 425°C. The pattern pertaining to sample (3a) reveals an amorphous phase with low crystallinity. However, peaks of the starting tetragonal MnO_2 precursor can also be observed in the XRD patterns (as identified by XRD card no. 81-2266) of spinels (1a) and (2a) having molar ratios of 0.75 and 1, respectively; as well as in the patterns of the adsorbents prepared via regime "b", but to a much lesser extent. This implies that raising the firing temperature leads to complete formation of the spinel. It can also be deduced from the figure that the intensity of the spinel peak gradually decreases with increasing the molar ratio which indicates that the best molar ratio that is suitable for the formation of the spinel is 0.75.

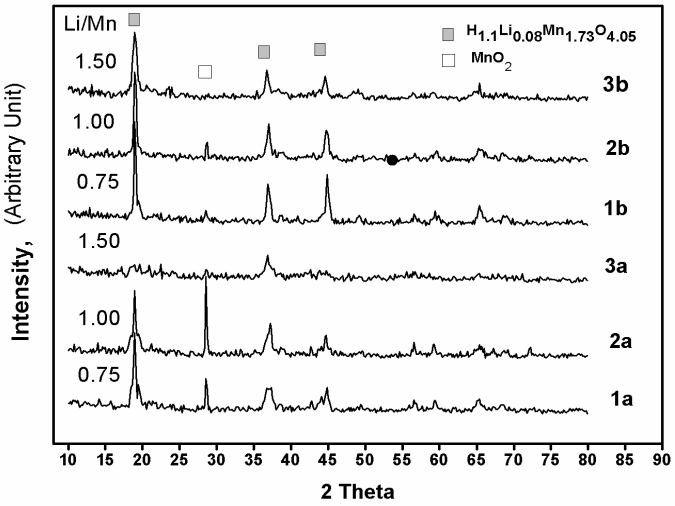

Fig. 2. XRD patterns for Group I spinel adsorbents prepared at different Li/Mn molar ratios.

The effect of the starting precursors on the formation and the structure of the spinels has been investigated. Figures 3A and 3B, respectively show the XRD patterns for Group IIA and Group IIB spinel adsorbents prepared via firing regimes "a" and "b" using the same Li/Mn ratio of 0.75 and different starting precursors of lithium ($LiOH.H_2O$ or Li_2CO_3) and manganese (MnO_2 or $MnCO_3$). The cubic face-centered spinel $H_{1.1}Li_{0.08}Mn_{1.73}O_{4.05}$ was also confirmed for all samples 4,5,6,7 of group II adsorbents. As can be seen in Fig. 3A and for Group IIA adsorbents, a peak for MnO_2 appears clearly only in the XRD pattern of spinel (4a) indicating incomplete formation of the spinel. In addition, it can be observed that the intensity of the spinel peaks increased noticeably when $MnCO_3$ was used as a starting precursor with lithium hydroxide as clear from the XRD patterns of spinels 5a and 5b. As for Group IIb adsorbents shown in Fig. (3B), the MnO_2 peak also appears only in the XRD pattern of spinel (6a). Furthermore, the use of two carbonate-based precursors (sample 7) produced spinels of lower crystallinity (7a and 7b) than that obtained with spinels using only one of the precursors in the carbonate form and the other in the oxide form (6a and 6b). In addition, the intensity of the spinel peak for (6b) is higher than (6a) indicating that all the starting precursors were consumed in the formation of the spinel upon rising the temperature.

It was found that the average crystal size of the prepared lithium manganese oxide spinels, as calculated from Scherrer equation, for group (I), (IIA) and (IIB) was in the range of 10-58 nm, 33-44 nm and 24-35 nm. It also noticed that incorporation of lithium and manganese carbonates decreases the resulting crystallite size.

From the above XRD analysis, it can be inferred that the cubic face-centered spinel $H_{1.1}Li_{0.08}Mn_{1.73}O_{4.05}$ was formed for all the prepared adsorbents except (3a) probably due to the combined effect of using high Li/Mn ratio and firing at a relatively low temperature (425^0C). However, the spinel was not completely formed for adsorbents 1a, 2a, 4a and 6a. This could probably be ascribed to the use of MnO_2 rather than $MnCO_3$ as a precursor, the former being a less reactive form of Mn. On the other hand, XRD patterns for spinels 5a, 5b, 7a and 7b prepared using $MnCO_3$ precursor with either precursors of Li ($LiOH.H_2O$ or Li_2CO_3) indicate complete formation of spinel. In addition, the intensity of the spinel peak and hence crystallinity is generally higher for spinels prepared using firing regime "b" than those prepared via regime "a". This could be due to employing relatively higher firing temperature and a slower cooling rate in regime "b". The slow cooling rate probably allowed for better crystal formation. The use of a Li/Mn ratio of 0.75 and a $MnCO_3$ precursor could thus be recommended for the preparation of spinels.

Spinels' morphology: SEM imaging

Scanning electron micrographs of selected lithium manganese oxide spinel adsorbents of each of Groups I and II are shown in Fig. 4. As can be seen, all the prepared lithium adsorbents are composed of cubic particles along with their

aggregates. The figure also shows the presence of rod shape that probably belongs to the tetragonal precursor MnO_2. The nanorods can thus be more clearly observed in adsorbents (1a), (1b), (2a) and (2b) where the XRD patterns showed that they still contain the precursor MnO_2. As for adsorbents (5a), (5b), (7a) and (7b), the morphology is mostly cubic due to the complete formation of spinel as confirmed by the XRD patterns. These results agree with other reported work [11,22,36].

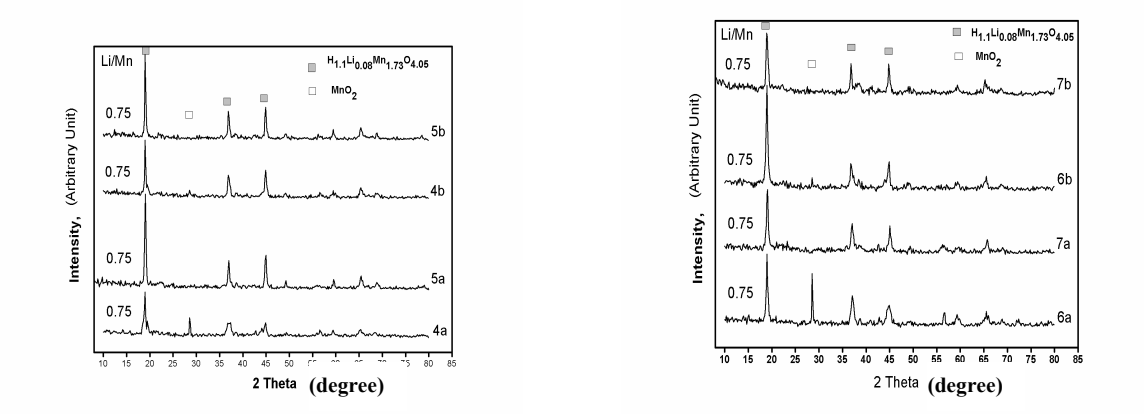

A)Group IIA **B) Group IIB**

Fig. 3. XRD patterns for Group II spinel adsorbents prepared at 0.75 Li/Mn molar ratio, A) Group IIA adsorbents and B) Group IIB adsorbents.

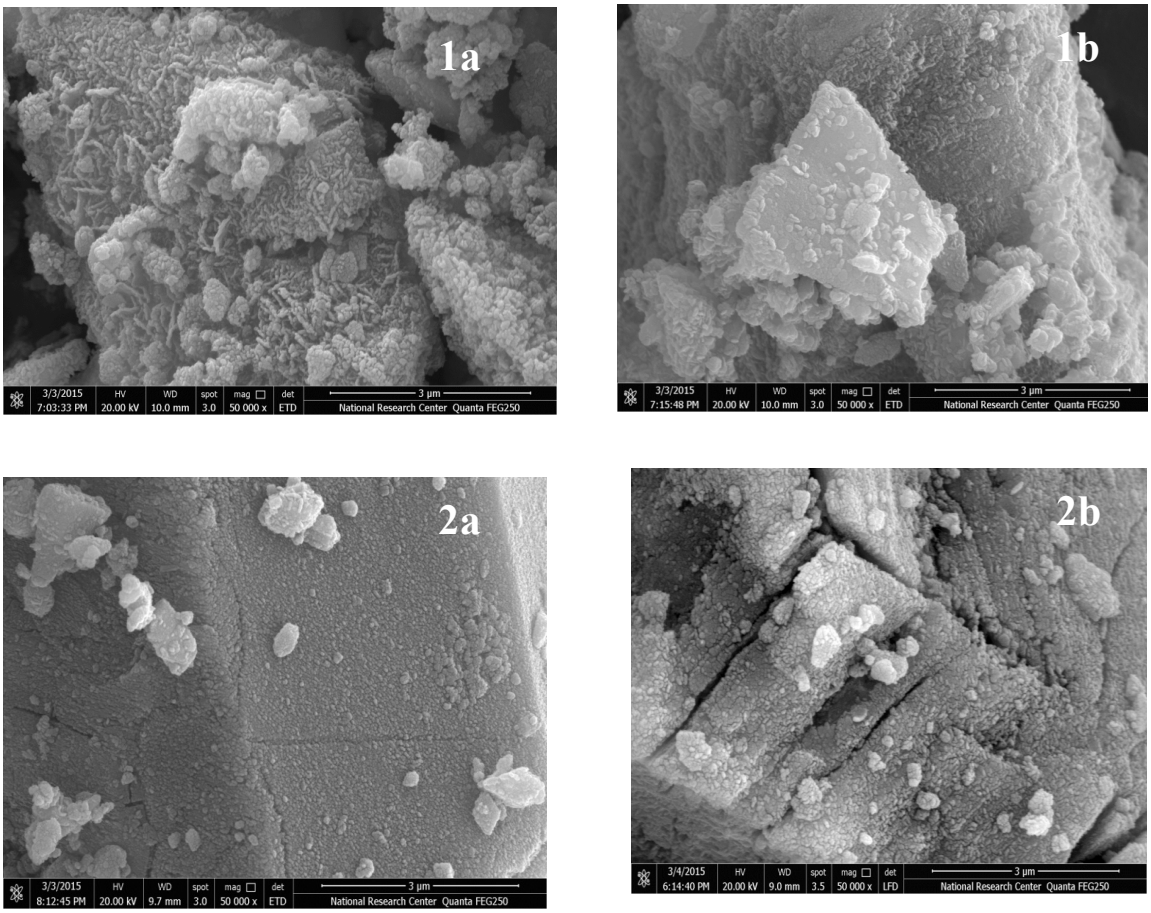

(A)

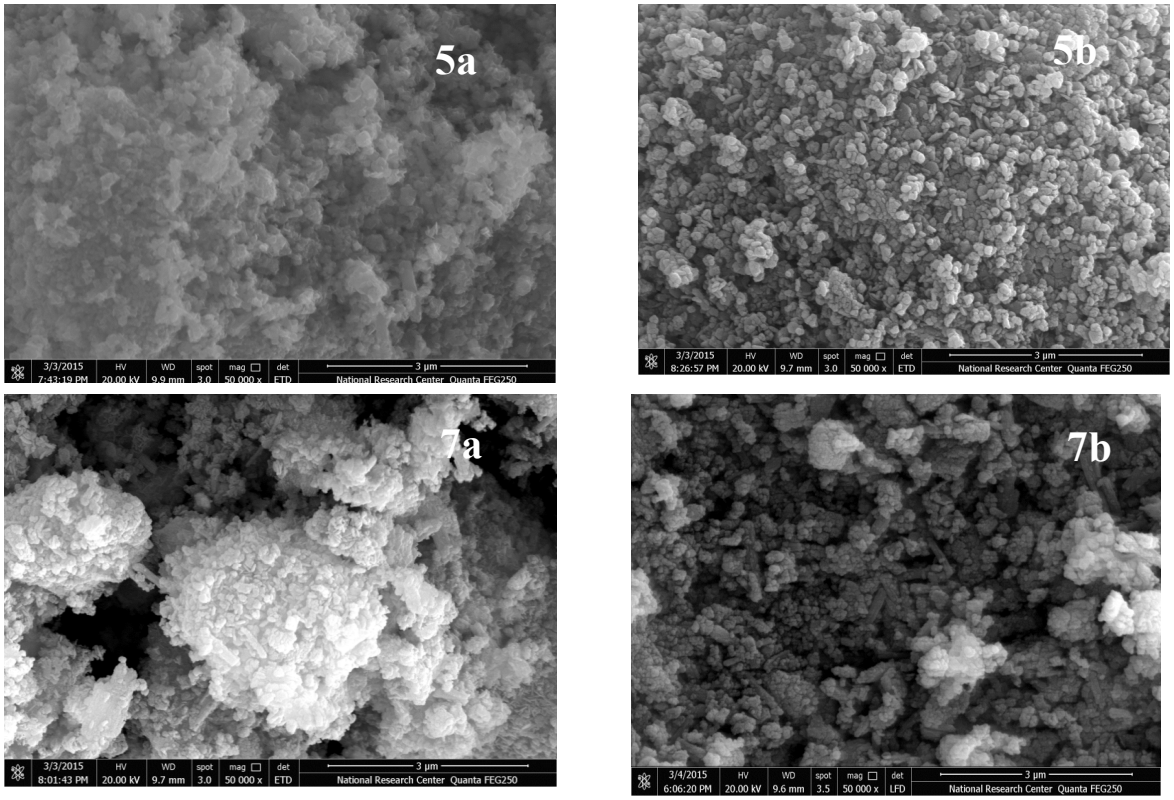

Fig. 4. SEM images for the prepared spinel adsorbents, A) group I and B) group II (scale bar is 3 µm).

Preliminary performance evaluation

Sorption capacities for the different prepared adsorbents were evaluated. Sorption was conducted at pHs 8 and 12 using 0.1 g adsorbent in 100 ml of 45 mg/L lithium chloride solution. These two pH values were chosen such that pH 8 mimics the pH of seawater, while pH 12 has been previously reported to yield high Li sorption capacities for spinel based adsorbents [15, 18]. In what follows, factors influencing sorption performance of each group will be discussed in separate subsections.

Group I adsorbents

Influence of Li/Mn starting molar ratio

Figure 5A depicts sorption capacities of samples 1, 2 and 3 at pH 8 and 12, which were prepared via firing regime "a". Among these adsorbents and as observed from the figure, adsorbent (3a) prepared using Li/Mn molar ratio of 1.5 exhibited the highest lithium sorption capacity (4.4 mg/g) at pH 8, which may be attributed to the amorphous phase of the spinel. While, adsorbent (1a) prepared using Li/Mn molar ratio of 0.75 exhibited the highest lithium sorption capacity (12.1 mg/g) at pH 12. This may be attributed to the presence of MnO in samples 1a and 2a as shown by XRD which decreased the sorption capacity of the samples especially at lower pH.

Figure 5B shows sorption capacities for Group I adsorbents (samples 1, 2 and 3) prepared via firing regime "b" fired at 500 C. Clearly, sample (1b) prepared using Li/Mn molar ratio of 0.75 exhibited the highest lithium sorption capacity (12.6 mg/g) at pH 8; whereas adsorbent (2b) prepared using Li/Mn molar ratio of 1.00 showed the highest sorption capacity (11.1 mg/g) at pH 12 with 24% removal efficiency. For regime "b" and at pH 8, the figure also shows that the sorption capacity decreases with increasing Li/Mn molar ratio which does not hold true for pH 12. For regime "a", there is, however, no clear trend for pH 8, while an inverse proportionality between sorption capacity and ratio is observed at pH 12.

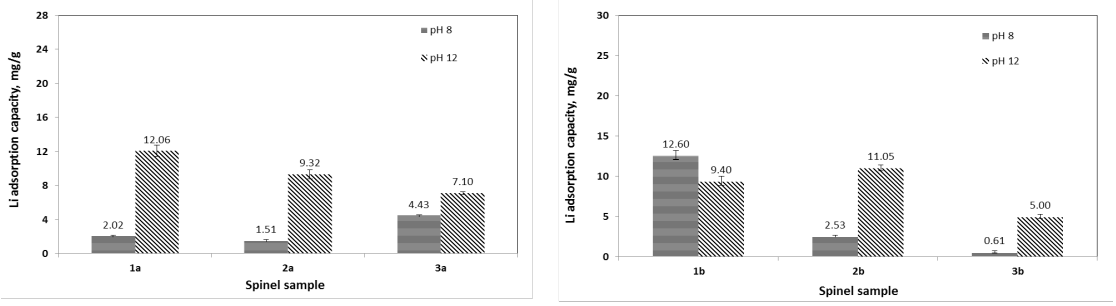

Fig. 5. Lithium sorption capacities at pH 8 and 12 for Group I adsorbents prepared via firing regime A) "a" and B) "b".

Influence of firing regime

Regarding the adopted firing regimes, it can be deduced from Fig. 5A and B that at pH 8, all Group I adsorbents prepared via firing regime "b" exhibited better lithium sorption capacities than their counterparts prepared via regime "a"; except for adsorbent (3a) where the spinel was not formed as shown earlier by XRD.

Furthermore, amongst all group I adsorbents, adsorbent (1b) yielded the highest sorption capacity of 12.6 mg Li/g at pH 8. At pH 12, on the other hand, adsorbents prepared via firing regime "a" were more favorable than their "b" counterparts since they yielded higher sorption capacities. This is in exception to adsorbent (2b). The Group I adsorbent with the highest sorption capacity at this pH (12) is adsorbent (1a) with a capacity of 12.1 mg Li/g.

In terms of sorption capacities, adsorbent (1b) prepared using the least employed Li/Mn ratio of 0.75 is the most favorable amongst other group I adsorbents. It showed a sorption capacity of 12.6 mg/g at pH 8 and removal efficiency of 27%.

Group II adsorbents

Influence of manganese precursor source

Figure 6A and B show the sorption capacities at pHs 8 and 12 for Group IIA adsorbents prepared via regime "a" and "b", respectively using two manganese-based precursors with $LiOH.H_2O$ at fixed Li/Mn molar ratio of 0.75. It is clear from Fig. 6A that for the adsorbents prepared via firing regime "a", adsorbent (5a) prepared using $MnCO_3$ exhibited higher lithium sorption than adsorbent (4a) with capacities of 7.8 mg/g and 21.5 mg/g at pH 8 and 12, respectively. It is also clear from Fig. 6B that adsorbent (4b) prepared using MnO_2 showed favorable lithium sorption than adsorbent (5b) with a capacity of 12.6 mg/g at pH 8. However, adsorbent (5b) prepared using $MnCO_3$ was more favorable than (4b) as it showed a sorption capacity of 14.96 mg/g and a removal efficiency of 32% at pH 12.

Also, shown in Fig. 6A are the sorption capacities for Group IIB adsorbents prepared using two manganese-based precursors with Li_2CO_3 at fixed Li/Mn molar ratio of 0.75. It is clear from the figure that for Group IIB adsorbents prepared via firing regime "a", adsorbent (7a) prepared using $MnCO_3$ exhibited better sorption performance than 6a where it showed capacities of 7.4 and 19.3 mg/g at pH 8 and 12, respectively. For the adsorbents prepared via firing regime "b", Fig. 6B shows that adsorbent (7b) is more favorable than (7a) since it exhibited sorption capacities of 9.8 and 13.4 mg/g at pH 8 and 12, respectively. The corresponding removal efficiencies were 21 and 29%, respectively.

Influence of firing regime

Regarding the adopted firing regimes, it can be deduced from Fig. 6A and B that Group IIA adsorbents prepared via regime "a" manifest higher sorption capacities at pHs 8 and 12 than those prepared via regime "b", except for adsorbents (4a) and (4b) at pH 8. From the above, it can be concluded that the highest lithium sorption capacity for Group IIA adsorbents was obtained at pH 12 using adsorbent (5a) prepared using $MnCO_3$ and $LiOH.H_2O$.This adsorbent showed a sorption capacity of 21.5 mg/g and removal efficiency of 48%.

Concerning the adopted firing regimes for group IIB samples, it can be deduced from Fig. 6A and 6B that at pH 12, samples prepared via firing regime "a" (6a) and (7a) exhibited better lithium

sorption capacities than their "b" counterparts (6b) and (7b). The opposite holds true for the same adsorbents at pH 8. In conclusion, the most favorable adsorbent of Group IIB is adsorbent (7a) prepared using $MnCO_3$ and Li_2CO_3. The adsorbent exhibits a sorption capacity of 19.3 mg/g and 43% removal efficiency.

From the above investigations, it can thus be concluded that higher lithium sorption capacities were obtained for the adsorbents prepared via firing regime "a" at both employed pH values. The use of a two-step firing regime similar to that of regime "b" has been previously reported in literature [27] and was employed to obtain $Li_xMn_2O_4$ spinels. In this study, however, it was possible to obtain spinels with high sorption capacity and using the low firing temperature regime "a". Among all the prepared adsorbents, the highest sorption capacities were obtained at pH 12 for adsorbent (5a) (21.46 mg/g) prepared from $LiOH.H_2O$ and $MnCO_3$, and adsorbent (7a) (19.3 mg/g) prepared using $MnCO_3$ and Li_2CO_3. The two adsorbents (5a) and (7a) have comparable sorption capacities at both pH 8 and pH 12. It has to be noted herein that the XRD results for these two adsorbents indicated complete formation of the spinels. In addition, it was found that using $MnCO_3$ precursor resulted in better sorption performance, especially when combined with $LiOH.H_2O$. The values of the obtained sorption capacities are comparable with those of Wang et al. [23] and Kitajou et al. [3] who obtained sorption capacities of 23 mg/g and 12-16 mg/g at pH 8, respectively. Accordingly, the electron dispersive spectrum (EDS) of selected spinel (5a) was examined. The EDS spectrum, Figure 7 shows very strong signals for O and Mn (main spinel elements). No detection of lithium or hydrogen was observed since they are difficult to detect by EDS analysis due to their small atomic sizes.

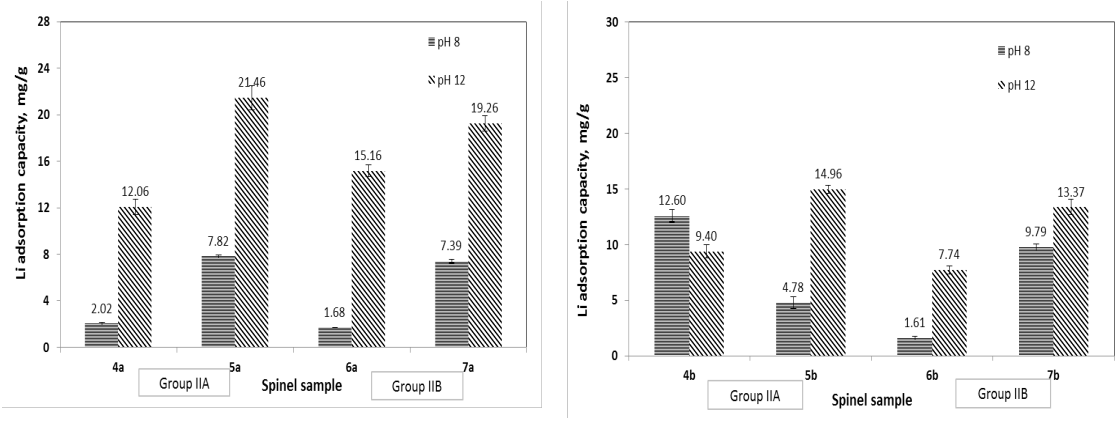

Fig. 6. Lithium sorption capacities at pH 8 and 12 for Group II adsorbents prepared via firing regime A) "a" and B) "b".

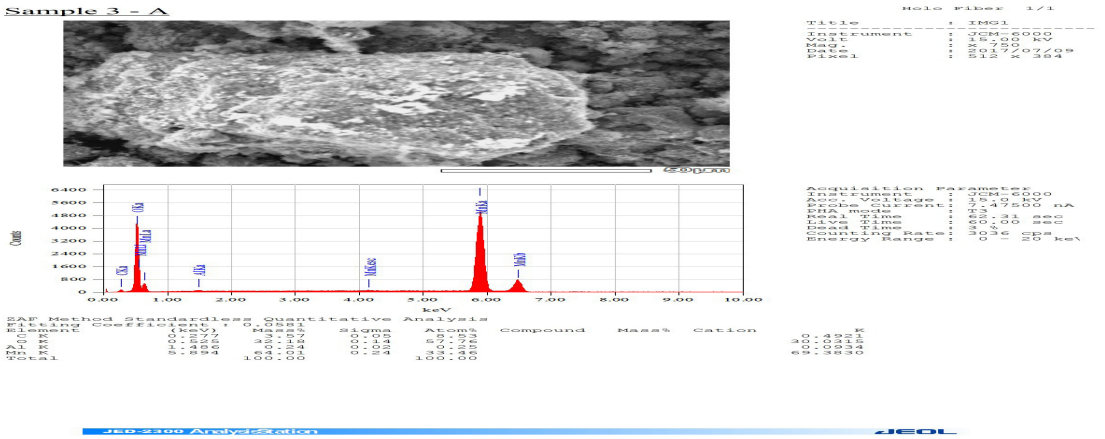

Fig. 7. Electron dispersive spectrum (EDS) of the prepared spinel adsorbent (5a).

Zeta potential and zeta sizing measurements

To gain more insight into the factors affecting sorption at the tested pH values, average particle size and zeta potential were measured for the two most favorable adsorbents (5a) and (7a) and the two adsorbents with the least sorption capacities (2a) and (3b). Table 2 compiles values thereof at pH 7, 8 and 12. For all adsorbents, particle size decreases while charge negativity increases with increasing the pH. The increase in the negative charge of the particles could have increased the repulsion forces between them and hence led to better dispersion and consequently smaller particle size. As shown earlier, better sorption capacities for all adsorbents were achieved at the higher pH of 12.This could be owed to the smaller particle size and the higher charge negativity at this pH. The smaller size provides larger surface area for sorption, while the high negative charge allows for better electrostatic interaction with lithium ions. Values of the average particle size for adsorbents (5a) and (7a) are respectively 733 and 702 nm at pH 8 as well as 511 and 437 nm at pH 12, while charge negativity values are -107 and -118 mV at pH 8 as well as -116 and -131 mV at pH 12.These values are statistically close within a 15% maximum error. As a result, sorption capacities for (5a) and (7a) adsorbents are comparable as deduced earlier.

Furthermore, adsorbents (5a) and (7a) possess higher sorption capacities than the others, for example adsorbents (2a) and (3b), which could be due to their smaller particle size. The charge negativities for adsorbents (5a) and (7a), however, are not necessarily higher than adsorbents (2a) and (3b). This is because the former adsorbents are composed mostly of spinel structures, whereas the latter adsorbents constitute other phases. To compare sorption behavior of these adsorbents that have different structures and morphologies, charge density will have to be considered.

Spinel dose effect

Based on the findings of section 3.2, spinel (5a) is considered the spinel that possesses the highest lithium adsorption capacity at pH 8 (7.82 mg/g) and pH 12 (21.46 mg/g). Accordingly, its dose was varied between 0.25-1 g/L lithium chloride solutions at pH 12 and 45 mg Li /L and the results are shown in Fig. 8. It is confirmed that decreasing the spinel (5a) dose resulted in increasing the lithium adsorption capacity from 21.46 mg/g to 41.5 mg/g indicating its increased ability for lithium uptake.

TABLE 2.Average particle size and zeta potential values for selected adsorbents at pH 7, 8 and 12.

	Average particle size (d.nm)			Zeta-potential (mV)		
	pH 7	**pH 8**	**pH 12**	**pH 7**	**pH 8**	**pH 12**
5a	1039	733.2	510.9	+ 0.185	-107	-116
7a	849.9	702.4	436.8	-26.2	-118	-131
2a	1546	972.7	585.6	-2.25	-75.0	-175
3b	960	887.2	791.5	-10.1	-85.1	-142

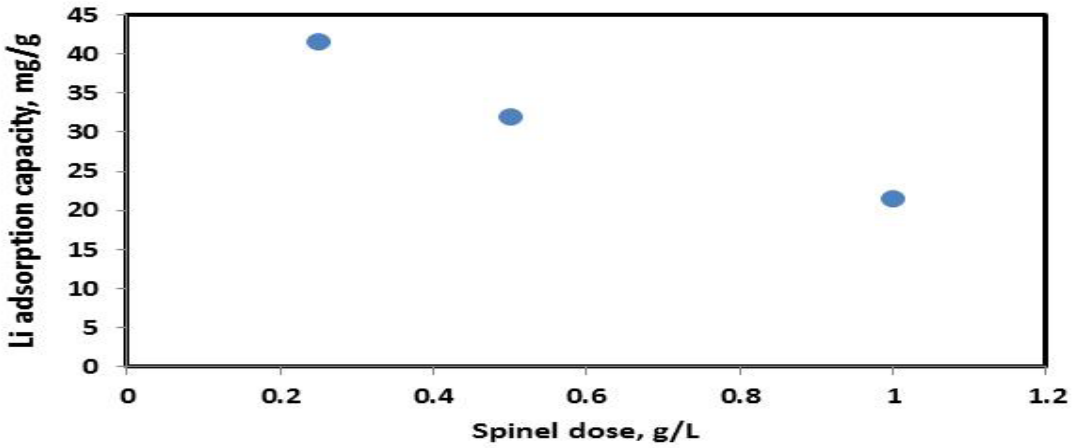

Fig. 8. Spinel (5a) dose effect on Li sorption capacity at pH 12 and different initial concentrations.

Equilibrium studies

Based on the findings of the previous sections, sorption behavior for the most favorable adsorbent (5a) was further investigated at the optimum dose. Figure 9 illustrates the effect of Li initial ion concentration on the sorption capacity using 0.25 g/L of the adsorbent (5a) at pH 12 for a range of initial concentrations ranging from 5 to 51 mg/L. It is clear that sorption capacity of Li ions increases linearly with increasing initial ion concentration. Capacity increased from 15 to 45 mg/g with increasing initial Li concentration by about 10 fold (from 5 to 51 mg/L). This increase could be owed to increasing the metal ion concentration gradient which overcomes mass transfer resistance. As shown in Fig. 9, the corresponding removal efficiencies declined from 80 to 21% by increasing Li ion initial concentration. The equations describing the relation between the initial concentration, C_o, and each of the sorption capacity, q, and the percent removal are shown in the figure.

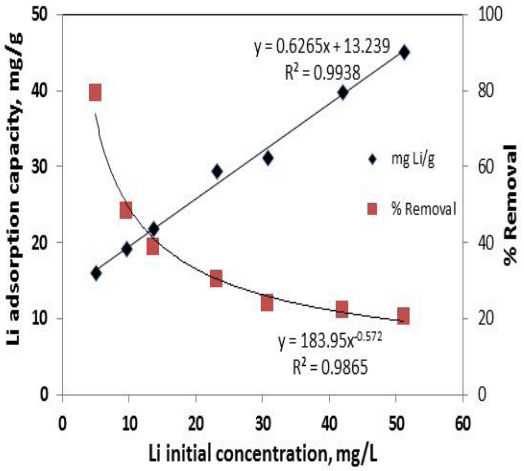

Fig. 9. Sorption capacity and removal efficiency of Li onto 0.25 g/L of the most favorable adsorbent (5a) at pH 12 and different initial concentrations.

To determine the maximum equilibrium Li sorption capacity for adsorbent (5a), isotherms pertaining to the sorption of Li ions onto the adsorbent at pH 12 and 28±2°C are depicted in Fig. 10. Data fitted to both Langmuir and Freundlich isotherm models are also shown.

Sorption parameters and correlation factors obtained from the slopes and intercepts of linear plots pertaining to Langmuir and Freundlich models are compiled in Table 3. As evident from R^2 values, lithium sorption can be better described by Langmuir rather than Freundlich model. This indicates monolayer coverage of ions on the outer surface of adsorbent (5a), with maximum equilibrium sorption capacity (q_m) of 50 mg/g. These results agree with reported work [15, 17, 18]. Table 4 presents values of the maximum equilibrium sorption capacities (q_m) reported in previous literature for manganese oxide based Li adsorbents, along with the value obtained in this study which is higher than the other reported values.

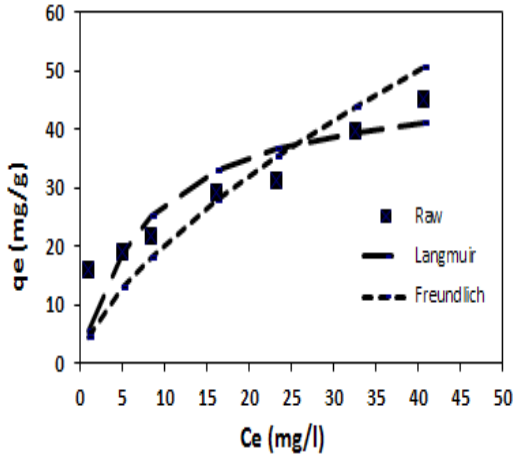

Fig.10. Sorption isotherms of Li ions onto the prepared spinel adsorbent (5a) at pH 12 and 28±2°C. The dashed lines represent data fitted by Langmuir and Freundlich isotherm models.

TABLE 3. Langmuir and Freundlich isotherm parameters for the sorption of Li ions onto the prepared spinel adsorbent (5a) at pH 12 and 28±2°C.

Isotherm	
Langmuir	
q_m (mg/g)	50.0
B (L/g)	0.123
R^2	0.930
Freundlich	
K_F((mg/g)/(L/mg)^n)	13.8
n	3.57
R^2	0.90

TABLE 4. Maximum equilibrium sorption capacities as reported in literature, along with maximum value obtained in this study.

adsorbent	pH/temperature(°C)	q_m, mg/g	reference
PAN (20%) -$H_{1.6}Mn_{1.6}O_4$ Li ion sieves	11/25	10.7	[17]
MnO_2 nano crystals ion sieve	9/20	16.8	[13]
$LiMn_2O_4$ or Li_2MnO_3	11/25	25.0	[16]
PVC-$H_{1.6}Mn_{1.6}O_4$ Li ion sieve membrane	12/25	36.8	[18]
Ion sieve $H_{1.41}Li_{0.07}Mn_{1.65}O_4$	12/25	41.0	[15]
MnO_2nanorod	10/30	45.7	[14]
$Li_{1.33}Mn_{1.67}O_4$		35	[25]

Conclusions

Manganese oxide based spinels were prepared for selective lithium sorption from synthetic solutions. The adopted semi-dry solid state synthesis involving different combinations of manganese-based and Li-based precursors fired using two different firing regimes were performed. The prepared adsorbents were characterized by X-ray diffraction (XRD), scanning electron microscopy (SEM) and dynamic light scattering (DLS) measurements. Nano-sized cubic face-centered spinels of $H_{1.1}Li_{0.08}Mn_{1.73}O_{4.05}$ were obtained. Furthermore, preliminary performance evaluation showed that lithium sorption is better conducted at pH 12 than at pH 8 where higher sorption capacities are achieved due to the smaller average particle size (from 437 to 511 nm) and higher charge negativity of the adsorbent particles (from -131 to -116 mV) at this pH. In addition, the most favorable adsorbent was prepared using $LiOH.H_2O$ and $MnCO_3$ precursors under the low-temperature firing regime and it yielded the highest sorption capacity of 21.5 mg/g at pH 12, 45 mg/L initial concentration of lithium chloride and 1 g/L adsorbent dose. This could be attributed to the use of $MnCO_3$ precursor which supports the complete formation of the spinel as confirmed by the XRD results. Further studies were performed on this adsorbent. It was found that sorption capacity increases linearly with increasing initial concentration. Adsorption of Li was best described by Langmuir isotherm, indicating monolayer coverage of ions on the outer surface of the adsorbent with maximum equilibrium sorption capacity q_m of 50 mg/g at pH 12 and 0.25 g/L adsorbent dose. In view of the above, it was possible to prepare a novel spinel-type manganese oxide adsorbent via a modified synthesis method that utilizes a low-temperature firing regime with $MnCO_3$ as a precursor along with $LiOH.H_2O$. The prepared adsorbent could be a potential candidate for the selective sorption of lithium.

Acknowledgement

"This work was financially supported by the Science and Technology Development Fund (STDF) of Egypt, under grant number STDF/3991".

References

1. Yoshizuka, K., Kitajou, A. and Holba, M., Selective recovery of lithium from seawater using a novel MnO_2 type adsorbent III-benchmark evaluation, *Ars Separatoria Acta,* 78-85(2006) .
2. Somrani, A., Hamzaoui, A. and Pontie, M., Study on lithium separation from salt lake brines by nanofiltration (NF) and low pressure reverse osmosis (LPRO), *Desalination,* **317,** 184-192(2013)
3. Kitajou, A. Suzuki,T., Nishihama, S. and Yoshizuka, K., Selective recovery of lithium from seawater using a novel MnO_2 type adsorbent. II–Enhancement of lithium ion selectivity of the adsorbent, *Ars Separatoria Acta* 97-106(2003).

4. Hong, H.J., Park, I.S., Ryu, T., Ryu, J. Kim, B.G. and Chung, K.S., Granulation of $Li_{1.33}Mn_{1.67}O_4$ (LMO) through the use of cross-linked chitosan for the effective recovery of Li^+ from seawater, *Chemical Engineering Journal,* **234,** 16-22 (2013).

5. El-Sayed, M.M.H., Hani, H.A. and Sorour, M.H., Polymeric Ion Exchangers for the Recovery of Ions from Brine and Seawater, Chemical *Engineering & Process Techniques,* **2,** 1020-1025(2014).

6. Wen, X., Ma, P., Zhu,C., He, Q. and Deng,X., Preliminary study on recovering lithium chloride from lithium-containing waters by nanofiltration, *Separation and purification technology,* **49,** 230-236(2006).

7. Gang,Y., Shi, H., Liu,W., Xing, W. and Xu, N., Investigation of Mg^{2+}/Li^+ Separation by Nanofiltration, *Chinese Journal of Chemical Engineering,* **19,** 586-591(2011).

8. Hoshino,T., Development of technology for recovering lithium from seawater by electrodialysis using ionic liquid membrane, *Fusion Engineering and Design,* **88,** 2956-2959(2013) .

9. Hamzaoui, A., M'nif, A., Hammi, H. and Rokbani, R. Contribution to the lithium recovery from brine, *Desalination* **158,** 221-224 (2003).

10. Ohya,H., Suzuki, T. and Nakao, S., Integrated system for complete usage of components in seawater: A proposal of inorganic chemical combinat on seawater, *Desalination* **134,** 29-36(2001).

11. Tian, L., Ma, W. and Han, M., Adsorption behavior of Li^+ onto nano-lithium ion sieve from hybrid magnesium/lithium manganese oxide, *Chemical Engineering Journal,* **156,** 134-140(2010).

12. Sorour, M.H., Hani., H.A. and Al-Bazedi, G.A., El-Sayed, M.M.H. Towards lithium recovery from seawater via an innovative Integrated Separation Process, *Desalination and Water Treatment* **61** 311–318(2017).

13. Zhang, Q.H., Sun, S., Li, S., Jiang, H. and Yu, J.G., Adsorption of lithium ions on novel nanocrystal MnO_2, *Chemical Engineering Science,* **62** 4869-4874(2007).

14. Zhang, Q.H., Li, S.P., Sun,S.Y., Yin,X.S. and Lithium, J.G. Yu, selective adsorption on 1-D MnO 2 nanostructure ion-sieve, *Advanced Powder Technology* **20,** 432-437 (2009).

15. Wang, L., Meng, C.G. and Ma,W., Study on Li+ uptake by lithium ion-sieve via the pH technique, Colloids and Surfaces A: *Physicochemical and Engineering Aspects,* **334,** 34-39(2009).

16. Shiu, J.Y., Lin, J.R., Lee, D.C., Chen,Y.M. and Liu, C.C., Method for adsorbing lithium ions from a lithium-containing aqueous solution by a granular adsorbent, *US Patent* No. / 0231996 A1(2003).

17. Park, M.J., Nisola, G.M., Beltran, A.B., Torrejos,R.E.C., Seo, J.G., Lee, S.P., Kim, H., and Chung, W.J., Recyclable composite nanofiber adsorbent for Li^+ recovery from seawater desalination retentate, *Chemical Engineering Journal,* **254,** 73-81 (2014).

18. Zhu, G.,Wang,P., Qi, P. and Gao, C., Adsorption and desorption properties of Li^+ on PVC-$H_{1.6}Mn_{1.6}O_4$ lithium ion-sieve membrane, Chemical *Engineering Journal,* **235,** 340-348(2014).

19. Zhang, Q.H., Li, S.P., Sun,, S.Y., Yin, X.S. and Yu, J.G., Lithium selective adsorption on low-dimensional titania nanoribbons, *Chemical Engineering Science,* **65,** 165-168(2010).

20. Lemaire, J., Svecova, L., Lagallarde,F., Laucournet, R. and Thivel, P.X., Lithium recovery from aqueous solution by sorption/desorption, *Hydrometallurgy,* **143,** 1-11 (2014).

21. Zhang,Q.H., Li,S.P., Sun, S.Y., Yin, X.S. and Yu, J.G., $LiMn_2O_4$ spinel direct synthesis and lithium ion selective adsorption, *Chemical Engineering Science,* **65,** 169-173(2010) .

22. Chitrakar, R., Kanoh, H., Miyai, Y., Ooi, K., A New Type of Manganese Oxide (MnO_2. 0.5 H_2O) Derived from Li1. 6Mn1. 6O4 and Its Lithium Ion-Sieve Properties, *Chemistry of Materials,* **12** 3151-3157(2000).

23. Wang, L. ,W. Ma, W., Liu, R., Li, H.Y. and Meng,C.G. Correlation between Li^+ adsorption capacity and the preparation conditions of spinel lithium manganese precursor, *Solid State Ionics* **177** 1421-1428(2006) .

24. Wang, L., Meng, C.G., Han, M. and Ma, W., Lithium uptake in fixed-pH solution by ion sieves, *Journal of Colloid and Interface Science,* **325,** 31-40 **(**2008).

25. Kim, Y.S., Moon, W.J., Jeong, S.K., Won, D.H. Lee, S.R. Byoung-Gyu Kim and Kang-Sup Chung, Synthesis of $Li_{1.6}[MnM]_{1.6}O_4$ (M=Cu, Ni, Co, Fe) and Their Physicochemical Properties as a New Precursor for Lithium Adsorbent, *Journal of the Korea Academia-Industrial Cooperation Society* ,**12,** 4660-4665 (2011).

26. Chitrakar, R., Kanoh,H., Miyai,Y. and Ooi, K., Recovery of lithium from seawater using manganese oxide adsorbent ($H_{1.6}Mn_{1.6}O_4$) derived from Li1. 6Mn1. 6O4, *Industrial & Engineering Chemistry Research,* **40,** 2054-2058(2001).

27. Yoshizuka, K., Fukui,K. and Inoue,K., Selective recovery of lithium from seawater using a novel MnO_2 type adsorbent, *Ars Separatoria Acta,* 79-86(2002).

28. Hwang, B.J.,Santhanam, B.J. R. and Liu, D.G., Characterization of nanoparticles of $LiMn_2O_4$ synthesized by citric acid sol–gel method, *J. Power Sources,* **97,** 443-446(2001).

29. Wu, S.H. and Chen, H.I., The effects of heat-treatment temperature on the retention capacities of spinels prepared by the Pechini process, *J. Power Sources,* 119–121, 134-138 (2003).

30. Sorour, M.H., EL-Rafei, A.M. and Hani, H.A.,Synthesis and characterization of electrospun aluminum doped $Li_{1.6}Mn_{1.6}O_4$ spinel, Ceramics International 42, 4911–4917 (2016)

31. Tuncer, C. and Recai, I., Determination of the competitive adsorption of heavy metal ions on poly (n-vinyl-2-pyrrolidone/acrylic acid) hydrogels by differential pulse polarography, *Journal of Applied Polymer Science,* **89,** 2013-2018 (2003).

32. Perry, R.H. Perry's Chemical Engineers' Handbook ((7th ed.), McGraw-Hill 1997.

33. Fogler, H.S., *Elements of Chemical Reaction Engineering*,3rd edition, Prentice-Hall PTR, New Jersy, 1999.

34. El-Rahman, K.M. , El-Kamash, A., El-Sourougy, M., Abdel-Moniem,N. , Thermodynamic modeling for the removal of Cs^+, Sr^{2+}, Ca^{2+} and Mg^{2+} ions from aqueous waste solutions using zeolite A, *Journal of Radioanalytical and Nuclear Chemistry,* **268** 221-230(2006).

35. Hani, H.A., Studies on zeolites for heavy metals removal, *PhD Thesis,* Cairo University, Egypt 2010.

36. Zandevakili,S., Ranjbar, M. and Ehteshamzadeh,M., Recovery of lithium from Urmia Lake by a nanostructure MnO 2 ion sieve, *Hydrometallurgy,* **149** ,148-152(2014) .

(*Received :*12/10/ 2016;
acecpted : 7/ 8/ 2017)

تحضر و توصيف و اختبار الأداء لإسبنيلات أكاسيد الليثيوم و المنجنيز لادمصاص الليثيوم

محمد حسن سرور، هبه أحمد هاني، ميادة محمد حسنس السيد، أماني عبدالمنعم مصطفى، هيام فهيم شعلان

قسم الهندسة الكيميائية و التجارب نصف الصناعية، المركز القومي للبحوث ،
قسم الكيمياء ، الجامعة الأمريكية بالقاهرة، القاهرة الجديدة، مصر و
قسم المواد الحيوية ، المركز القومي للبحوث، الدقي، الجيزة، مصر

يعتبر استرجاع الليثيوم من مياه البحر عن طريق الامتزاز من تقنيات الفصل الواعدة و التي يمكن إدراجها ضمن خطط متكاملة لاستعادة الملح. في هذا البحث، تم تحضير ممتزات أكسيد المنغنيز من نوع الإسبنيل واستخدامها لامتزاز الليثيوم الانتقائي من المحاليل المخلقة. تم التحضير باستخدام طريقة الحالة الصلبة شبه الجافة باستخدام مصادر مختلفة من المنجنيز والليثيوم؛ كربونات المنجنيز، أكسيد المنجنيز، كربونات الليثيوم وهيدروكسيد الليثيوم. كما تم التحصير باستخدام نسب مولية بادئة مختلفة من الليثيوم/المنجنيز، ودرجاتحرارة و أزمنة احتراق مختلفة. وعلاوة على ذلك، تم قياس .(SEM) والمجهر الإلكتروني المسح (XRD) وقد تم اخبار خصائص الإسبنيل باستخدام حيود الأشعة السينية متوسط حجمالجسيماتو جهدالزيتالممتزاتالإسبنيلالمختارة. وبالإضافةإلىذلك،تمتقييمقدراتالامتزازوالكفاءةلإزالةالليثيوم من المحاليل المخلقة. المعد من كربونات المنجنيز وهيدروكسيد الليثيوم باستخدام (H1.1Li0.08Mn1.73O4.05) وأظهرت نتائج ادمصاص الليثيوم أن الإسبنيل نسب مولية بادئة الليثيوم/المنجنيز0،75 و معرض الى درجة الحموضة 12 أعلى قدرة امتصاص الليثيوم بين الاسبنيلات المعدة الأخرى. و تم وتم التوصلالى أقصى قدر من الادمصاص 50 ملجم / لتر. تم الحصول على هذهLangmuir تمثيل اتزان ادمصاص الليثيوم من قبل نموذج القدرة باستخدام 0.25 جم / لتر من الممتزات عند الرقم الهيدروجيني 12 وتعتبر هذه القيمة أعلى من القيم المعلنة سابقا. وهكذا، فإن الإسبنيل المحضرة يظهر سمات واعدة تحبذ استخدامه في إزالة الليثيوم من المياه العادمة والمحاليل الملحية المركزة.